JBC Papers in Press. Published on November 16, 2012 as Manuscript M112.386441
The latest version is at http://www.jbc.org/cgi/doi/10.1074/jbc.M112.386441

Anticoagulant activity of a unique sulfated pyranosic (1→3)-β-L-arabinan through direct interaction with thrombin*

Paula V. Fernández[1], Irene Quintana[2], Alberto S. Cerezo[3,§], Julio J. Caramelo[4,§], Laercio Pol-Fachin[5], Hugo Verli[5,6], José M. Estevez[7,§], Marina Ciancia[1,3,§]

From the [1]Cátedra de Química de Biomoléculas, Departamento de Biología Aplicada y Alimentos, Facultad de Agronomía, Universidad de Buenos Aires, Av. San Martín 4453, 1417 Buenos Aires, Argentina.
[2]Laboratorio de Hemostasia y Trombosis, Departamento de Química Biológica, Facultad de Ciencias Exactas y Naturales, Universidad de Buenos Aires, Ciudad Universitaria – Pabellón 2, C1428EHA Buenos Aires, Argentina.

[3]CIHIDECAR-CONICET, Departamento de Química Orgánica, Facultad de Ciencias Exactas y Naturales, Universidad de Buenos Aires, Ciudad Universitaria, Pabellón 2, C1428EHA Buenos Aires, Argentina.
[4]Instituto de Investigaciones Bioquímicas de Buenos Aires (IIBBA), CONICET, Av. Patricias Argentinas 435, 1405 Buenos Aires, Argentina.
[5]Programa de Pos-Graduação em Biologia Celular e Molecular, Centro de Biotecnologia, Universidade Federal do Rio Grande do Sul, Brasil.
[6]Faculdade de Farmácia, Universidade Federal do Rio Grande do Sul, Brasil.
[7]Instituto de Fisiología, Biología Molecular y Neurociencias (IFIByNE-CONICET), Facultad de Ciencias Exactas y Naturales, Universidad de Buenos Aires, Ciudad Universitaria – Pabellón 2, C1428EHA Buenos Aires, Argentina.

*Running title: *Sulfated arabinan from Codium with direct effect on thrombin*

To whom correspondence should be addressed: Marina Ciancia, Cátedra de Química de Biomoléculas, Departamento de Biología Aplicada y Alimentos, Facultad de Agronomía, Universidad de Buenos Aires, Av. San Martín 4453, 1417 Buenos Aires, Argentina. Tel.: +54 11 4524-4042, Fax: +54 11 4524-8088. E-mail: ciancia@agro.uba.ar.

Keywords: sulfated arabinan; arabinopyranose; green seaweed; anticoagulant activity; thrombin-polysaccharide interaction

Background: Many seaweed polysaccharides have anticoagulant activity, but the mechanism of action was elucidated in a few cases.
Results: A highly sulfated pyranosic β-arabinan exerts its activity through direct and indirect inhibition of thrombin.
Conclusion: The structure and mechanism of action of the arabinan are different to those found for other polysaccharides.
Significance: This arabinan could be an alternative anticoagulant in certain specific cases.

SUMMARY

A highly sulfated 3-linked β-arabinan (Ab1) with arabinose in the pyranose form was obtained from green seaweed *C. vermilara* (Bryopsidales). It comprised major amounts of units sulfated on C-2 and C-4, and constitutes the first polysaccharide of this type isolated in the pure form and fully characterized. Ab1 showed anticoagulant activity by global coagulation tests. Less sulfated arabinans obtained from the same seaweed, have less or no activity. Ab1 exerts its activity through direct and indirect (antithrombin- and heparin cofactor II-mediated) inhibition of thrombin. Direct thrombin inhibition was studied in detail. By native PAGE it was possible to detect formation of a complex between Ab1 and human thrombin (HT). Ab1 binding to HT was measured by fluorescence spectroscopy. CD spectra of the Ab1-complex suggested that ligand binding induced a small conformational change on HT. Ab1-thrombin interactions were studied by molecular dynamic simulations using the persulfated octasaccharide as model compound. Most carbohydrate-protein contacts would occur by interaction of sulfate groups with basic amino acid residues in the surface of the enzyme,

being more than 60% of them performed by the exosite 2-composing residues. In these interactions the sulfate groups on C-2 showed to interact more intensely with thrombin structure. In contrast, the disulfated oligosaccharide does not promote major conformational modifications at the catalytic site when complexed to exosite 1. These results show that this novel pyranosic sulfated arabinan Ab1 exerts its anticoagulant activity by a mechanism different to those found previously for other sulfated polysaccharides and glycosaminoglycans.

Codium species biosynthesize a complex system of sulfated polysaccharides. Love and Percival (1964) (1) reported that the water-soluble polysaccharides from *C. fragile* were composed, at least in part, by 3-linked galactopyranose and 3-linked arabinopyranose units, the former being sulfated on C-4 or C-6, while the arabinose residues were suggested to carry sulfate either on C-2 or C-4. Later, it was found that the room temperature water-extracts of *C. fragile* and *C. vermilara* were constituted by a family of sulfated polysaccharides comprising galactose and arabinose as major components (2,3). Results obtained until now did not allow to establish beyond doubt whether they are arabinogalactans, or a mixture of arabinans and galactans. A lot of information has been obtained in recent years about the galactan structures, which were isolated in some cases in a pure form (2-6) with some small variations on the structures for different species, however, information about the arabinan moiety is scarce (2,3,7,8).

Many different sulfated polysaccharides from seaweeds were found to have anticoagulant activity. The important differences in their mechanisms of action could be attributed to the diversity of structures and to the fact that one compound may have more than one target protease. These differences illustrate the importance of the knowledge of specific structural characteristics of these products and their interaction with the different proteins involved in coagulation cascade in order to understand the regulation of the coagulation process and for developing new antithrombotic therapeutic agents (9). Sulfated polysaccharides from several *Codium* species showed anticoagulant activity (10). This effect was usually attributed to potentiation of antithrombin (AT) and/or heparin cofactor II (HCII). However, a proteoglycan from *C. pugniformis* showed both direct and AT mediated inhibition for thrombin activity (11). On the other hand, sulfated polysaccharides from other *Codium* species exhibited thrombin inhibition by a HCII-dependent pathway with higher effectiveness than that of heparin or dermatan sulfate and this effect was more potent for sulfated arabinans than for sulfated galactans (7). The driving force for the formation of the sulfated polysaccharide/protein complex was attributed to a non-specific polar interaction between the negatively and positively charged groups in the polysaccharide and protein, respectively. The complex would be further stabilized by short-range interactions (9).

In a previous paper, we reported the characterization of an extract from *C. vermilara* with high anticoagulant activity inferred from global coagulation tests (APTT, TT) (2). We report now the isolation of an arabinan and its structural characterization as a unique highly sulfated (1→3)-β-L-arabinan, with the arabinose units in the pyranose form, as well as the analysis of its anticoagulant behavior, focusing on direct thrombin inhibition mechanism.

EXPERIMENTAL PROCEDURES

Algal sample-Samples of *Codium vermilara* were collected in San Antonio Oeste (Río Negro, Argentina). They were identified according to ref. (12). A voucher material was deposited in the herbarium of the Bernardino Rivadavia Museum, Buenos Aires, Argentina (collection number 40466).

Isolation of the sulfated arabinans-**Ab1** was obtained by fractionation of the room temperature water extract of *Codium vermilara* (2) with potassium chloride. The raw polysaccharides (0.5 g) were dissolved in water (250 ml, 0.25 %). Solid, finely divided KCl was added to the supernatant in small portions with constant and violent mechanical agitation so that the concentration was increased by 0.005-0.05 M each time. After each addition, stirring was continued for 3-5 h to ensure equilibration of the system. The upper limit of KCl concentration was 2.0 M. The precipitate, obtained at 0.115 M (**Ab1**, 31 % p/p of the parent extract), as well as the residual solution were dialyzed (MWCO 3,500), concentrated and freeze-dried. By a similar procedure a precipitate was obtained at 0.1 M concentration of this salt from the hot water extract of the same seaweed (2). This product was highly contaminated with amylose, so it was submitted to a treatment with α-amylase (13), and then fractionated again by addition of KCl to give a 0.1 M concentration, obtaining arabinan **Ab2**

(5.1 % p/p of the hot water extract). A stepwise addition of NaCl to a solution of the room temperature water extract of *Codium vermilara* up to 2 M yielded no precipitate.

Chemical analyses-The total sugars content was analyzed by phenol-sulfuric acid method (14). Sulfate was determined turbidimetrically (15). The protein content was determined colorimetrically (16). Optical rotations (Na D-line) were measured in a Perkin–Elmer 343 polarimeter, using 0.2–0.4 % solutions of the polysaccharides in water. For GC, alditol acetates were obtained by reductive hydrolysis and acetylation of the samples (17). Number average molecular weight was estimated by the method of Park & Johnson (18).

Desulfation-The reaction was carried out by the microwave-assisted method described by Navarro et al. (19). **Ab1** (20 mg) was converted to the pyridinium salt and dissolved in 10 ml of DMSO containing 2 % of pyridine. The mixture was heated for 10 s intervals and cooled to 50 ºC (x 6). It was dyalized a week against tap water and then 2 days against distilled water (MWCO 3,500) and lyofilized (yield 69 %, considering the sulfate loss). An aliquot was methylated as described bellow without previous isolation of the product.

Methylation analysis-The polysaccharide (5-10 mg) was converted into the corresponding triethylammonium salt (17) and methylated according to Ciucanu & Kerek (20); finely powdered NaOH was used as base. The methylated derivative was hydrolyzed and the partially methylated sugars were derivatized to the alditol acetates (17).

Gas Chromatography-GC of the alditol acetates were carried out on a Hewlett Packard 5890A gas-liquid chromatograph (Avondale PA, USA) equipped with a flame ionization detector and fitted with a fused silica column (0.25 mm i.d. x 30 m) WCOT-coated with a 0.20 μm film of SP-2330 (Supelco, Bellefonte PA, USA). Chromatography was performed from 200 °C to 230 °C at 1 °C min $^{-1}$, followed by a 30-min hold for alditol acetates. For the partially methylated alditol acetates, the initial temperature was 160 ºC, which was increased at 1 ºC min^{-1} to 210 ºC and then at 2 ºC min^{-1} to 230 ºC. N_2 was used as the carrier gas at a flow rate of 1 ml min $^{-1}$ and the split ratio was 80:1. The injector and detector temperature was 240 °C.

GC–MS-GC–MS of the methylated alditol acetates was performed on a Shimadzu GC-17A gas-liquid chromatograph equipped with a SP-2330 column interfaced to a GCMSQP 5050A mass spectrometer (Kyoto, Japan) working at 70 eV. The total He flow rate was 7 ml min^{-1}, the injector temperature was 240 ºC. Mass spectra were recorded over a mass range of 30–500 amu.

FTIR spectroscopy-Fourier-transform infrared spectra were recorded from 4,000 to 250 cm^{-1} with a 510P Nicolet FTIR spectrophotometer (Madison WI, USA), using dry samples in KBr. 32 scans were taken with a resolution of 4 cm^{-1}. Data collection and processing were performed on the OMNIC 7.2 (Thermo-Nicolet, Madison, WI, USA).

NMR spectroscopy-Samples (15-20 mg) were dissolved in D_2O solutions (0.5 ml) and lyofilized, this procedure was repeated twice. Then, they were dissolved in D_2O, agitated 24 h at room temperature, and centrifuged. 500 MHz ^{1}H NMR, proton decoupled 125 MHz ^{13}C NMR spectra, and two-dimensional NMR experiments (HMQC and COSY) were recorded on a Bruker AM500 (Billerica, MA, USA) at room temperature, with external reference of TMS. Chemical shifts were referenced to internal acetone (δ_H 2.175, δ_{CH3} 31.1). Parameters for ^{13}C NMR spectra were as follows: pulse angle 51.4º, acquisition time 0.56 s, relaxation delay 0.6 s, spectral width 29.4 kHz, and scans 25,000. For ^{1}H NMR spectra: pulse angle 76º, acquisition time 3 s, relaxation delay 3 s, spectral width 6250 Hz and scans 32. 2D spectra were obtained using standard Bruker software.

Fluorescence spectroscopy-Fluorescence spectra were measured with a Jasco FP-6500 spectrofluorimeter at 20 ºC in 10 mM Tris-HCl buffer, pH 7.4. Samples containing 1 μM HT were titrated with a concentrated solution of polysaccharide in a 4x4 mm quartz cell. After incubation for 5 min, the samples were excited at 295 nm and emission was recorded in the range 300-430 nm. Spectral slit widths were set to 1 and 5 nm, respectively. Each spectrum is the average of 6 scans. In each case, the blank was subtracted and data were corrected for dilution. Binding affinity was estimated by fitting a Hill cooperative binding model to the fluorescence intensity at 335 nm ($F = F_0 + \Delta F.[L]^n / (Kd + [L]^n)$), where F is the measured signal, F_0 is the signal in the absence of polysaccharide, ΔF is the signal change at protein saturation with polysaccharide, Kd is the dissociation constant and n is the Hill coefficient).

Circular dichroism spectroscopy-Circular dichroism (CD) spectra were measured with a Jasco J-815 spectropolarimeter. All spectra were

taken at 20 °C in 10 mM Tris-HCl buffer, pH 7.4. Spectra were recorded using 1 mm path cell in the range 190-260 nm. Each spectrum is the average of 15 scans. For these experiments, we employed 2 μM HT and/or 10 μM polysaccharide.

General coagulation assays-They were performed with a coagulometer ST4 (Diagnostica Stago, Asnières sur Seine, France). Determinations of prothrombin time (PT), activated partial thromboplastin time (APTT), and thrombin time (TT) were assayed according to established methods (21). Reagents were supplied by Diagnostica Stago, except purified bovine thrombin (Wiener, Rosario, Argentina). Normal platelet depleted citrated plasma (900 μl) was mixed with 100 μl of each polysaccharide sample, in different concentrations, and incubated for 1 min at 37 °C. Heparin (Sigma, USA) and dermatan sulfate (Syntex, Buenos Aires, Argentina) were used for the comparison of anticoagulant activity of the fractions. Saline solution (0.9 % NaCl) was used as control. TT-like assays were also performed with purified fibrinogen (3 mg/ml) instead of plasma. All clotting assays were performed in quadruplicate. Results were expressed as ratios obtained by dividing the clotting time achieved with the anticoagulant by the time achieved with the control.

Amydolytic assays-Amydolytic assays were performed according to the method of Colliec et al. (22). 50 μl of polysaccharide solution (5-100 μg/ml) in Tris-HCl buffer, pH 7.4 containing 7.5 mM EDTA and 150 mM NaCl were mixed with 75 μl of AT or HCII (200 nM) (Diagnostica Stago). After 2 min incubation at 37 °C, 75 μl of thrombin solution (10 U/ml for bovine thrombin, or an equivalent concentration for human thrombin determined by TT assay) were added and the mixture was incubated at 37 ° C for 1 minute. Then, 75 μl of chromogenic substrate S-2238 1.5 mM (Chromogenix, Milan, Italy) was added and absorbance at 405 nm was measured with a Stat Fax 303 microstrip reader. It is important to note that bovine thrombin (BT) was used in AT potentiation assays, and HT was used in the case of HCII, because of its specificity. Direct inhibition of thrombin activity by the polysaccharides was determined by the same assay as described above, but incorporating buffer in place of AT or HCII solutions. A non-competitive partial inhibition model was fitted to inhibition data ($Vmax' = Vmax. (1 + \beta[I]/Ki) / (1 + [I]/Ki)$, where Vmax' is the measured activity, Vmax is the activity in the absence of polysaccharide, Ki is the thrombin-polysaccharide dissociation constant and β is the fraction of residual activity under saturation conditions.

Electrophoresis-The ability of sulfated arabinan to modify the migration pattern of thrombin was evaluated by native and denaturing polyacrylamide gel electrophoresis (SDS-PAGE). Equal volumes of purified thrombin (165 NIH/ml) and Ab1 (250 μg/ml) were incubated for 30s at room temperature and the reaction was stopped by addition of electrophoresis sample buffer, followed by heating at 100 °C for 5 min in the case of SDS-PAGE. Electrophoresis was performed in a 4-15 % precast polyacrylamide gel for use with Mini-PROTEAN Tetra Cell (BioRad, Richmond, CA, USA). Proteins were stained with 0.25 % Coomassie Blue R-250 in 40 % methanol and 10 % acetic acid, and sulfated polysaccharides were visualized with 1 % (w/v) Toluidine Blue *O* (pH=6.8).

Docking procedures-Structures of HT and BT were retained from PDB IDs 1PPB and 1TBQ, respectively (23,24). Both disulfated ([L-Ara*p***2,4S-**(1→3)-L-Ara*p***2,4S**]$_4$) and non-sulfated arabinan ([L-Ara*p*-(1→3)-L-Ara*p*]$_4$) octasaccharides were constructed based on the most prevalent conformations of their composing disaccharides, obtained from solution MD simulations, as previously described (25,26). For these calculations, the pyranosic arabinose was only considered in its most abundant form, that is, $^4C_1$. For the docking studies, protein and carbohydrate structures were prepared with AutoDockTools 1.5.4 for AutoDock 4.2 (27), using AutoGrid to generate grid dimensions and parameters to cover exosites 1 and 2, each in separated runs, of both thrombin structures. The Lamarckian Genetic Algorithm was applied, with default parameters, except for the maximum number of generations in each run (set to 270,000) and the number of generated docked conformations, set to 1,000, after 100 docking runs. Orientations of the oligosaccharides were selected based on binding energy, abundance of orientations and superimposition with heparin on a cluster of a 2.0 Å cutoff.

MD simulations-Both HT and BT were simulated in four conditions: (a) uncomplexed, (b) complexed to the non-sulfated arabinan in exosite 2, (c) complexed to the disulfated arabinan in exosite 2 and (d) complexed to the disulfated arabinan in exosite 1, in a total of eight simulations. Each of these systems was solvated

in triclinic boxes using periodic boundary conditions and SPC water model. The Lincs method (28) was applied to constrain covalent bond lengths, allowing an integration step of 2 fs after an initial energy minimization using Steepest Descents algorithm. Electrostatic interactions were calculated with Particle Mesh Ewald method (29). Temperature and pressure were kept constant at 310 K and 1.0 atm by coupling proteins, oligosaccharides, ions and solvent to external temperature (30) and pressure (31) baths with coupling constants of $\tau = 0.1$ and 0.5 ps, respectively. The dielectric constant was treated as $\varepsilon = 1$. The systems were heated slowly from 50 to 310 K, in steps of 5 ps, each one increasing the reference temperature by 50 K. After this heating, all simulations were further extended to 50 ns under a constant temperature of 310 K. All simulations were performed under GROMACS simulation suite, version 4.0.5 (32) and GROMOS96 43a1 force field (33). In the case of thrombin-arabinan complexes, before data collection, 10 ns MD simulations were employed as equilibration, with an initial 5000 kJ mol^{-1} restraining applied to both protein and carbohydrate. This constant force was reduced by 1000 kJ mol^{-1} at every 2 ns, allowing water molecules and counter-ions to settle around the complexes.

RESULTS

Structural studies-The room temperature water extract from green seaweed *C. vermilara* (2) was stepwise fractionated with potassium chloride producing one sharp precipitation at 0.115 M KCl (**Ab1**). **Ab1** is a highly sulfated arabinan, which contains 97 % of L-arabinose and 54.1 % of sulfate (as SO_3K), giving a sulfate:arabinose molar ratio of 1.8:1.0, $[\alpha]_D$ = + 167.5 º, and number average molecular weight of 180 kDa; only traces of proteins were detected. **Ab1** was desulfated giving **DAb1**, which still contained 5.2 % of sulfate and $[\alpha]_D$ = + 50.3 º. In addition, a similar, but less sulfated arabinan (43.7 %, sulfate:arabinose molar ratio 1.5:1.0) was isolated from the hot water extract of the same seaweed by an equivalent procedure (**Ab2**).

Methylation analysis of **Ab1** showed major amounts of arabinose and 2-*O*-methylarabinose, with lesser but still significant quantities of 4-*O*-methylarabinose and 2,4-di-*O*- methylarabinose, showing that 3-linked 2,4-disulfated, 2- and 4-monosulfated, and non-sulfated arabinopyranose units are present (**Table 1**). The same structural units are present in **Ab2**, but in different quantities. The percentage of arabinose units sulfated on C-4 is similar; however, it has less than half of the disulfated units, while the amount of non-sulfated units is important. Methylation analysis of **DAb1** showed 88 % of 2,4-di-*O*-methylarabinose (**Table 1**) in agreement with the (1→3)-linkages suggested above and confirming that most of the units in the native product are 2,4-disulfated.

FTIR spectrum of **DAb1** showed only absorptions which correspond to the carbohydrate backbone (**Fig. S1).** The region 855-830 cm^{-1} was previously reported as useful to distinguish between β- and α-arabinopyranose, because the former absorbs in this range, while IR spectrum of the latter shows no absorptions in this zone (34). In **DAb1**, a small peak at 835 cm^{-1} was observed, and it was the first evidence of a β-configuration of the arabinopyranose units. Sulfate groups give also peaks in this region, absorptions at 855 and 825 cm^{-1} in **Ab1** were assigned to stretching of C4-O-S (axial) and C2-O-S (equatorial), respectively (35). In **DAb1**, no peaks were found at ν ~1226-1275 cm^{-1} corresponding to the O=S=O asymmetric stretching vibration, while there is a strong signal in this region in the spectrum of **Ab1**, in agreement with previous chemical analysis.

HMQC spectra of **Ab1** and **DAb1** are shown in **Fig. 1**. Only five major carbon signals were detected in the spectrum of **Ab1** (**Table 2, Fig. 1A**). The β-L-configuration of the anomeric carbon was confirmed from the signal at 97.0 ppm in the spectrum of **DAb1**. The displacement of the anomeric signal in 1.5 ppm to higher fields in the spectrum of **Ab1** is in agreement with well known effect of the sulfate group at C-2 (36,37). Similar results were found for a 2-sulfated α-L-galactan (38) and a 2-sulfated α-L-fucan (39), in which the configuration is similar to that of this arabinan (**Fig. S2**). Moreover, experimental and *ab initio* calculated $J_{H,H}$ coupling constants for H1-H2 and H2-H3 for galactans and fucans, which have similar configuration, confirmed a preferred $^4C_1$ conformation for the arabinose pyranose ring (40). Besides, the signal at 61.6 ppm, which corresponds to C-5 of these units (41) confirms this assignment considering that an axial sulfate group on C-4 produces a small displacement to higher fields of the C-5 carbon signal (36). The displacement of C-2 and C-4 are those expected for substitution with sulfate groups, and that of C-3 of the influence of the glycosidic linkage. Minor peaks could correspond to non-sulfated units.

The spectrum of **DAb1** also shows five major carbon peaks (**Fig. 1B**) assigned to 3-linked β-L-arabinopyranose units, considering the values reported for the signals of methyl β-D-(β-L) and α-D-(α-L) arabinopyranosides (41,42), of 3-*O*-L-arabinopyranosyl-L-arabinose (43), of the non-reducing (1→3)-β-L-arabinopyranose unit from an oligosaccharide (44), and of the effects of glycosylation in disaccharides with pyranose aglycone having the equatorial proton at one of the β-carbons (45).

Both anomeric signals in the ^{1}H NMR spectra of **Ab1** and **DAb1** (5.37 ppm, doublet, J 1.5-2.5 Hz, unresolved) and 5.12 ppm, doublet J 2.3 Hz, respectively) are in agreement with a β-L-arabinopyranosidic unit in a $^{4}C_{1}$ chair conformation; the displacement to lower fields of the anomeric proton of **Ab1** respect to that of **DAb1** is in agreement with sulfation on C-2.

Spectra of **Ab2** show the same major peaks as those of **Ab1**, plus two signals at 4.03/69.5 and 4.57/73.7 ppm, which were tentatively assigned to H-2/C-2 and H-3/C-3, respectively of 3-linked arabinopyranose units sulfated only on C-4. These results confirmed that **Ab1** is constituted by major amounts of 3-linked β-L-arabinopyranose disulfated units. In **DAb1**, these units are mostly non-sulfated, while in **Ab2**, there are important quantities of disulfated units, but also mono-sulfated on C-4.

Anticoagulant activity of the arabinans-Global clotting assays were performed on plasma incubated with **Ab1**, heparin or dermatan sulfate, respectively. No clotting inhibition was observed in PT with these samples at low concentrations. However, when the concentration of the polysaccharide was increased, longer PT were observed (**Table S1**). These results were attributed to the presence of polybrene in the commercial reagent (46). On the other hand, APTT and TT were prolonged in a concentration dependent manner and the anticoagulant activity proved to be lower than that of heparin and somewhat higher than that of dermatan sulfate (**Table S1**). In addition, **Ab1** was compared with **Ab2** and **DAb1 (Table S2)**. The anticoagulant effect of these arabinans which have the same backbone, showed to be determined, as expected, by the degree of sulfation, being **Ab1** the most active arabinan. In addition, coagulation time was determined with **Ab1** and human thrombin (HT) or bovine thrombin (BT), using the same conditions and reagents of TT assay but with purified fibrinogen instead of plasma (**Table S3**). A significant prolongation of TT was observed for both thrombins in these conditions, although this effect was more important for BT.

Besides, there was a decrease in amydolytic activity of thrombin in the presence of increasing concentrations of **Ab1**. With HT and BT of equal coagulant activity determined by TT, BT showed a greater decrease in its amydolytic activity (**Fig. 2A**); that is, **Ab1** exerted a higher inhibition effect on BT. A partial non-competitive inhibition model was fitted to inhibition curves This procedure rendered a thrombin-**Ab1** inhibition constant of 62 and 19 μM for HT and BT, respectively. The residual activity extrapolated at saturating concentration of **Ab1** was 57 % for HT and 32 % for BT.

In order to establish comparisons, not in terms of concentration, but in terms of effect, the APTT value obtained for a concentration of 5 μg/ml of **Ab1** (2.5-3 times the coagulation time of the control) was set up as starting point. Then, "equivalent" concentrations of heparin and dermatan sulfate that prolonged APTT in a similar way were determined. These concentrations of **Ab1**, heparin and dermatan sulfate (5.0, 0.65 and 9 μg/ml, respectively) were used in amydolytic assays (**Table S4**). As expected no direct inhibition of thrombin was observed with heparin and dermatan sulfate.

Interaction between human thrombin and **Ab1** was assessed by native and SDS-PAGE (**Fig. 3**). When purified HT (~38kDa) was incubated with **Ab1**, no changes were observed in its migration pattern in SDS-PAGE (**Fig. 3A**), as a unique protein band was visualized with Coomasie Blue (CB). Besides, a high molecular weight band (~180 kDa) corresponding to **Ab1** was visualized by staining with Toluidine Blue *O* (TB*O*). On the other hand, when native PAGE was performed on HT incubated with **Ab1** (**Fig. 3B)**, a cathodic shift with regard to the bands corresponding to **Ab1** and HT was detected with both TB*O* and CB staining suggesting the formation of a stable complex HT-**Ab1**.

When physiological inhibitors (AT or HCII) were added to the system, **Ab1** induced an inhibition even greater on thrombin amydolytic activity. In both cases, the polysaccharide potentiated inhibitor effect on thrombin in a concentration-dependent way **(Fig. 2B).** Compared to direct thrombin inhibition assays, there was an additional loss in residual thrombin activity. Thus, at a concentration of 5 μg/ml of **Ab1** the decrease in residual thrombin activity was ~50% (54.3% ± 5.3 to 24.1% ± 0.9 for AT and BT, and 84.2% ± 3.6 to 43.5% ± 5.9 HCII

and HT). On the other hand, in the same experimental conditions the decrease in residual thrombin activity for heparin at the equivalent concentration (0.65 μg/ml) was ~73 % for AT and ~60 % for HCII.

Biophysical characterization of Ab1-thrombin complex-Binding of **Ab1** to HT was studied by fluorescence spectroscopy **(Fig 4A)**. Mature HT displays 9 Trp residues placed at different environments. For this reason, the emission spectrum of HT showed a broad band with a maximum at 335 nm. The addition of **Ab1** induced a 2 nm redshift of the emission maximum and an increment of about 20 % of the fluorescence intensity (**Fig. 4A**). A cooperative binding model described by the Hill equation was fitted to the fluorescence intensity at 345 nm (**Fig. 4B**), yielding a Kd of 17 ± 3 μM with a cooperative coefficient n of 2.1 ± 0.2.

Structural changes upon complex formation were explored by circular dichroism in the far-UV. The spectrum of HT displayed features of alpha helix and beta sheet (**Fig. 4C**). Deconvolution of this spectrum with the program CDSSTR using the basis SP37 rendered a content of 16.5 % alpha helix and 31 % beta sheet. These values are in close agreement from those calculated from the pdb file 1PPB of HT (15 % alpha helix and 36 % beta sheet). Polysaccharide addition induced a small change in the CD spectrum of thrombin. Interestingly, the spectrum of the complex cannot be completely described as the addition of spectra of the isolated components, suggesting that either HT or **Ab1** or both suffered a conformational change upon binding.

Modelling Ab1-thrombin interactions by molecular dynamic (MD) simulation-Considering that the conformational preferences of carbohydrates may be accessed through their composing glycosidic linkage geometries, the disaccharide units within the arabinan structures were conformationally evaluated by relaxed contours plots, followed by a solution MD refinement (**Fig. S3**). From these data, it was observed that the non-sulfated disaccharide showed an additional minimum-energy region when compared to its sulfated counterpart. On the other hand, in solution both glycosidic linkages showed a similar major conformational state, centered at $\phi = 90^{o}$ and $\psi = -120^{o}$. Based on this geometry, the octasaccharide fragments for those arabinans were built and employed as ligands during the docking procedures. Accordingly, the orientations obtained for the disulfated and non-sulfated arabinan octasaccharides on the surface of both BT and HT enclosed thrombin exosite 2, mostly superimposing heparin arrangement on the surface of thrombin, as observed in previous crystal structures (47). Additionally, as sulfated compounds have been also described to bind exosite 1 (48), docking procedures of the disulfated oligosaccharides were also carried out at such region. Such complexes were further refined through MD simulations, from which data on the dynamics of thrombin-arabinan complexes was retrieved.

Accordingly, the binding of the disulfated arabinan oligosaccharide to exosite 2 of HT and BT affects the flexibility of several portions in the protein structure (**Figs. 5A-B**). Among these regions, those around residues 60 and 77, located in close vicinity to the thrombin active site, comprise loops whose plasticity is increased in the presence of the oligosaccharide. Additionally, considering that heparin binding to exosite 2 had been shown to influence the conformation of thrombin active site (49), such possibility was also evaluated for the disulfated arabinan, in which the distance between atoms His57 ND1 and Asp102 OD1, from the catalytic triad, was observed to increase in the presence of the disulfated oligosaccharide (**Figs. 5C-D**), in a disrupted conformational state (**Figs. 5E-F**). Such profile, while indicating a disturbance of the catalytic site organization, is in agreement with **Ab1** anticoagulant activity, stronger over BT when compared to HT (**Fig. 2A**).

The interaction between arabinan oligosaccharides and BT or HT indicates that most protein-carbohydrate contacts through sulfate groups are mediated by basic amino acid residues in the enzymes surface (**Table 3**), being more than 60 % of them performed by the exosite 2-composing residues, as identified in previous mutagenesis studies (50), and more intense for BT (**Table 3**), while the remaining contacts are mostly performed by other positively-charged amino acid residues. The main interaction differences between both thrombins and **Ab1** may originate from the C-terminal region of the enzymes, where three variant residues may be observed (HT *versus* BT): (1) Gln244 *versus* Arg244, which provides an additional basic amino acid residue for interaction with **Ab1** in BT; (2) Phe245 *versus* Leu245, which removes a bulky residue, which may facilitate accommodation of **Ab1** in the surface of BT; (3) Glu247 *versus* Ser247, which changes an acidic

amino acid residue, incapable of interacting with **Ab1** sulfate groups, by a polar one, which can contribute in this process donating a hydrogen bond. Additionally, in **Ab1**-thrombin complexes the 2-linked sulfate groups showed to interact more intensely with both thrombin structures than the 4-linked groups (**Table S5**). On the other hand, the non-sulfated arabinan octasaccharide has such interactions weakened or eliminated, although the interactions with exosite 2-composing residues were retained (**Table 3**). Also, the sulfate absence on such octasaccharide leads to changes of the non-sulfated arabinan orientation in relation to thrombin structure, when compared to the disulfated oligosaccharide (**Figs. 5E-F**).

In contrast, HT shows reduced global flexibility as due to the binding of disulfated arabinan oligosaccharide to exosite 1, while only point differences may be observed for BT, when compared to the uncomplexed enzymes. Such profile is maintained in the catalytic triad organization of both proteins, as evaluated for the distance between His57 ND1 atom and Asp102 OD1 atom. In other words, while complexation of the disulfated arabinan oligosaccharide to thrombin exosite 2 appears to be able to promote a conformational modification at the enzyme catalytic site, its complexation to exosite 1 does not promote major modifications in the enzymes dynamics (**Fig S4**).

DISCUSSION

The system of polysaccharides synthesized by green seaweed *C. vermilara* is constituted by major amounts of sulfated L-arabinans and sulfated D-galactans. Sulfated D-galactans in green seaweeds have been previously found in other species of *Codium* and their structure was determined (4-6, 51). Recently, a small amount of a sulfated mannan was also reported (52).

L-Arabinose is a constituent of many different cell wall components, including pectins, glucuronoarabinoxylans, arabinogalactan proteins, and extensins (53,54). Although the pyranose form of L-arabinose is thermodynamically more stable, in these polymers it occurs mostly in the furanose form. Terminal L-arabinopyranose has been reported on short branches of β-(1→6)-galactan of arabinogalactan-proteins (AGP) from different sources (55), some of the L-arabinopyranose units of wheat flour AGP were terminal, while other L-arabinopyranoses are substituted with L-arabinofuranose residues (56), but no longer sequence of L-arabinopyranose units has been found. Moreover, to the best of our knowledge, *Codium* species are the only known natural source of polymers constituted only by arabinopyranosic units. Based on these structural features, **Ab1** represents a unique arabinan reported for the first time.

Sulfated arabinans were obtained from several species of *Codium* (molar ratios sulfate/arabinose, 0.5-0.8), and their anticoagulant behavior was analyzed, but no structural details were determined (7). Two similar sulfated L-arabinans were isolated from *C. dwarkense* (8) and *C. latum* (57) by precipitation with 0.12 M and 0.2 M KCl, respectively and they were characterized as furanosic sulfated α-L-arabinans, the latter with (1→5)-linkages, without specification of the position of the sulfate groups. On the other hand, partial acid hydrolysis of the water-extract of *C. fragile* yielded 3-*O*-β-L-arabinopyranosyl-L-arabinose (1) and the arabinans deduced from structural analysis of the room-temperature water extracts from *C. fragile* and *C. vermilara*, and some of the fractions obtained from them, showed a linear backbone of 3-linked β-L-arabinopyranose units with major sulfate substitutions at C-2 and C-4 and minor at C-4, (2,3).

In this work, **Ab1** was isolated from the room temperature water extract of *C. vermilara* in an important yield through a sharp gelification at 0.115 M KCl. No precipitation occurred when using sodium chloride, indicating that the insolubilization is K^+-specific as in the case of κ-carrageenans. Lower or higher concentrations of potassium chloride (upper limit 2 M) did not show any other precipitation. This product is a linear 3-linked β-L-arabinopyran with major sulfation on both C-2 and C-4, and minor quantities of monosulfated units on C-4 or on C-2. The mechanism of gel formation in dilute potassium chloride solutions has been extensively studied for κ-carrageenan where junction zones in gels are formed by quaternary interactions at the superhelical level (58) between ordered tertiary structures (double helices), promoted by potassium ions, through the one-stage domain mechanism of aggregation (coil → double helix → gel) (59). It seems likely that a similar mechanism could explain gel formation of other polysaccharides in which the primary mode of interchain association is through multi-stranded helices (59,60). **Ab2**, less sulfated than **Ab1** also

precipitated with potassium chloride, but at a higher concentration (0.5 M).

Thrombosis is one of the principal causes of morbid-mortality in the world and heparin is one of the most commonly used drugs in antithrombotic therapy (61). Since heparin can induce several side effects, such as thrombocytopenia, arterial embolism, bleeding complications and others derived from its animal origin, like prion-related diseases (62) development of new anticoagulant drugs, and particularly direct thrombin inhibitors, is desirable (63).

Ab1 significantly increased APTT and TT in concentration dependent way with respect to the control. Prolongation of the APTT suggests inhibition of the intrinsic and/or common pathway of coagulation, meanwhile the strongly extended TT indicates either thrombin inhibition (direct or mediated by AT/HCII) or impaired fibrin polymerization. A TT-like assay was performed using purified fibrinogen instead of plasma. In this case, prolongation of the coagulation time was also observed and this was the first signal of a possible direct inhibition of **Ab1** on thrombin activity, taking into account that AT and HCII were absent in the test. Amydolytic assays in the absence of physiological inhibitors of thrombin confirmed our preliminary finding, since an important decrease in residual thrombin activity was obtained with **Ab1**. Direct inhibition of thrombin by **Ab1** was experimentally determined with both HT and BT and the effect was significantly higher in the latter case. These results are in agreement with molecular dynamic (MD) simulation analysis, since **Ab1** proved to induce a greater alteration in the catalytic triad of BT than in the case of HT. This alteration in the geometry of active site of thrombin could be related to the diminished activity of the enzyme on fibrinogen and chromogenic substrate observed in our results. In spite of the higher inhibition of BT by **Ab1**, interaction of HT and **Ab1** was studied in more detail due to its possible interest for human health.

Native polyacrylamide gel electrophoresis showed that **Ab1** forms a stable complex with HT in the experimental conditions used, as the top band that appeared when both molecules were incubated together contained protein and polysaccharide. In contrast, this complex was not observed in SDS-PAGE. These results confirm that, although interactions between **Ab1** and HT are strong enough to stabilize the complex for its observation in native-PAGE, no covalent interactions are established between these molecules. Besides, **Ab1** binding to HT was measured by changes of their intrinsic fluorescence spectrum. Ligand addition induced a redshift and an increment of HT emission, from which a Kd of 17 ± 3 μM can be calculated by using a cooperative binding model. The reasons underlying this behavior are not clear. Finally, CD spectra of the **Ab1**-complex suggested that ligand binding induced a small conformational change on HT, although we can not rule out the possibility that the differences observed could arise from changes on **Ab1** upon binding to HT.

Ab1 also produced potentiation of physiological inhibitors of thrombin: AT and HCII. The relative importance of these effects could not be clearly established, since both direct and indirect mechanisms (AT- or HCII-mediated) of inhibition of thrombin, were acting together in amydolytic assays. For both indirect mechanisms, when the physiological inhibitor was added to the assay, there was an additional loss in residual thrombin activity of ~50 %, compared to direct thrombin inhibition assays due to the inhibition through direct and indirect mechanisms (**Figs. 2A-B**). Although AT- and HCII-mediated inhibition of thrombin is reported here, we focused on the direct inhibition mechanism. Further research is required to elucidate how these additional effects work.

Regarding the relationship between structure and function, APTT and TT assays performed on **Ab1**, **Ab2**, and **DAb1** showed that less sulfated arabinans are less active. Although **Ab2** is still highly sulfated, in most of the monosulfated arabinose units, sulfate ester is on C-4. Thus, its weaker activity is in agreement with this structural feature, as it was shown that sulfate groups on C-2 seem to interact more intensely with structure of exosite 2 of thrombin, and with the fact, previously established, that the anticoagulant activity of polysaccharides is not merely a consequence of their sulfate content, but also of the sulfation pattern (9, 64). Interaction of **DAb1** with thrombin is too weak to change the activity of the enzyme. Such differences may be related both to the interaction energy intensities between the enzymes and the polysaccharides and to the different orientations of disulfated and non-sulfated arabinans in relation to thrombin. Direct thrombin inhibition was already reported for other sulfated polysaccharides from seaweeds, e.g., highly branched fucans from brown algae (39), ulvans from *Ulva conglobata* (65) and

galactans and proteoglycans from some other *Codium* species (11,51). However, no details about mechanisms of action at a molecular level for direct thrombin inhibition by seaweed sulfated polysaccharides were provided before.

Available direct thrombin inhibitors (DTIs) block thrombin interaction with its substrates by binding either to both the active site and exosite 1 (bivalent DTIs), or only to the active site (univalent DTIs) (63). On the other hand, heparin interacts with exosite 2 of thrombin, but it only inhibits the enzyme by an AT-dependent mechanism, meanwhile dermatan sulfate potentiates HCII without binding to thrombin. The unusual mechanism described in this paper for **Ab1**, direct thrombin inhibition by interaction with exosite 2 that alters active site without mediation of AT, could be of interest in the context of development of antithrombotic strategies targeting thrombin.

REFERENCES

1. Love, J. and Percival, E. (1964) The polysaccharides of the green seaweed *Codium fragile*: Part II. The water-soluble sulphated polysaccharides. *J. Chem. Soc.* 3338–3345.
2. Ciancia, M., Quintana, I., Vizcargüénaga, M. I., Kasulin, L., de Dios, A., Estevez, J. M., and Cerezo, A. S. (2007) Polysaccharides from the green seaweeds *Codium fragile* and *C. vermilara* with controversial effects on hemostasis. *Int. J. Biol. Macromol.* **41***,* 641–649.
3. Estevez, J. M., Fernández, P. V., Kasulin, L., Dupree, P., and Ciancia, M. (2009) Chemical and *in situ* characterization of macromolecular components of the cell walls from the green seaweed *Codium fragile*. *Glycobiology*, **19***,* 212-228.
4. Bilan, M. I., Vinogradova, E. V., Shashkov, A. S., and Usov, A. I. (2007) Structure of a highly pyruvylated galactan sulfate from the pacific green alga *Codium yezoense* (Bryopsidales, Chlorophyta). *Carbohydr. Res.* **342***,* 586–596.
5. Farias, E. H. C., Pomin, V. H., Valente, A. P., Nader, H. B., Rocha, H. A. O., and Mourão, P. A. S. (2008) A preponderantly 4-sulfated, 3-linked galactan from the green alga *Codium isthmocladum*. *Glycobiol*ogy **18**, 250–259.
6. Ohta, Y, Lee, J-B, Hayashi, K., and Hayashi, T. (2009) Isolation of Sulfated Galactan from *Codium fragile* and Its Antiviral Effect, *Biol. Pharm. Bull.*, **32**, 892-898.
7. Hayakawa, Y., Hayashi, T., Lee, J.-B., Srisomporn, P.;,Maeda, M.;,Ozawa, T., & Sakuragawa, N. (2000). Inhibition of thrombin by sulfated polysaccharides isolated from green seaweeds. *Biochim. Biophys. Acta,* **1543***,* 86-94.
8. Siddhanta, A. K., Shanmugam, M., Mody, K. H., Goswami, A. M., and Ramabat, B. K. (1999) Sulphated polysaccharides of *Codium dwarkense* Boergs. from the west coast of India: chemical composition and blood anticoagulant activity. *Int. J. Biol. Macromol.,* **26***,* 151–154.
9. Ciancia, M., Quintana, I., and Cerezo A. S. (2010) Overview of anticoagulant activity of sulfated polysaccharides from seaweeds in relation to their structures, focusing on those of green seaweeds. *Curr. Med. Chem.*, **17**, 2503-2529.
10. Jurd, K. M., Rogers, D. J., Blunden, G., and McLellan, D. S. (1995) Anticoagulant properties of sulphated polysaccharides and a proteoglycan from *Codium fragile* ssp. *atlanticum. J. Appl. Phycol.*, **7**, 339-45.
11. Matsubara, K., Matsuura, Y., Hori, K., Miyazawa, K. (2000) An anticoagulant proteoglycan from the marine green alga, *Codium pugniformis. J. Appl. Phycol.*, **12,** 9-14
12. Boraso de Zaixso, A. L. (2004) Marine Chlorophyta of Argentina. *Hist. Nat.* (Segunda Serie) **3**, 95-119.
13. Knutsen, S. H., and Grasdalen, H. (1987). Characterization of water extractable polysaccharides from norwegian Furcellaria umbricalis (Huds) Lamour (Gigartinales, Rhodophyceae) by IR and NMR spectroscopy. *Botanica Marina*, **30**, 497–505.
14. Dubois, M., Gilles, K. A., Hamilton, J. K., Rebers, P. A., and Smith, F. (1956) Colorimetric method of determination of sugars and related substances. *Anal. Chem.,* **28***,* 350–356.
15. Dodgson, K. S., and Price, R. G. (1962) A note on the determination of the ester sulphate content of sulphated polysaccharides. *Biochem. J.,* **84,** 106–110.
16. Lowry, O. H., Rosenbrough, N. J., and Farr, A. L. (1951) Protein measurements with the Folin phenol reagent. *J. Biol. Chem.,* **193,** 265–275.

17. Stevenson, T. T., and Furneaux, R. H. (1991) Chemical methods for the analysis of sulphated galactans from red algae. *Carbohydr. Res.,* **210***,* 277–298.
18. Park, J. T., and Johnson, M. J. (1949) A sub microdetermination of glucose. *J. Biol. Chem.*, **181**, 149–151.
19. Navarro, D. A., Flores, M. L., and Stortz, C. A. (2007) Microwave-assisted desulfation of sulfated polysaccharides. *Carbohydr. Pol.,* **69**, 742–747.
20. Ciucanu, I., and Kerek, K. (1984) A simple and rapid method for the permethylation of carbohydrates. *Carbohydr. Res.,* **134**, 209–217.
21. Laffan, M. A,, and Bradshaw, A. E. (1995) Investigation of haemostasis, in *Practical Haematology* (Dacie, J. V., and Lewis, S. M., eds). Churchill Livingstone, New York, pp. 297-315.
22. Colliec, S., Fischer, A. M., Tapon-Braudiere, J., Boisson, C., Durand, P., and Jozefonvicz, J. (1991) Anticoagulant properties of a fucoidan fraction. *Thromb. Res.* **64**, 143-154.
23. Bode, W., Mayr, I., Baumann, U., Huber, R., Stone, S.R., and Hofsteenge, J. (1989) The refined 1.9 Å crystal structure of human alpha-thrombin: interaction with D-Phe-Pro-Arg chloromethylketone and significance of the Tyr-Pro-Pro-Trp insertion segment. *EMBO J.,* **8***,* 3467-3475.
24. van de Locht, A., Lamba, D., Bauer, M., Huber, R., Friedrich, T., Kröger, B., Höffken, W., and Bode, W. (1995) Two heads are better than one: crystal structure of the insect derived double domain Kazal inhibitor rhodniin in complex with thrombin. *EMBO J.,* **14***,* 5149-5157.
25. Fernandes, C. L., Sachett, L. G., Pol-Fachin, L., and Verli, H. (2010) GROMOS96 43a1 performance in predicting oligosaccharide conformational ensembles within glycoproteins. *Carbohydr. Res.,* **345,** 663-671.
26. Pol-Fachin, L., Serrato, R. V., and Verli, H. (2010) Solution conformation and dynamics of exopolysaccharides from *Burkholderia* species. *Carbohydr. Res.,* **345***,* 1922-1931.
27. Morris, G. M., Huey, R., Lindstrom, W., Sanner, M.F., Belew, R.K., Goodsell, D.S., and Olson, A. J. (2009) AutoDock4 and AutoDockTools4: Automated docking with selective receptor flexibility. *J. Comput. Chem.,* **30**, 2785-2791.
28. Hess, B., Bekker, H., Berendsen, H. J. C., and Fraaije, J. G. E. M. (1997) LINCS: A Linear Constraint Solver for Molecular Simulations. *J. Comput. Chem.,* **18***,* 1463-1472.
29. Darden, T., York, D., and Pedersen, L. (1993) Particle mesh Ewald: An N-log(N) method for Ewald sums in large systems. *J. Chem. Phys.,* **98,** 10089-10092.
30. Berendsen, H. J. C., Postma, J. P. M., van Gunsteren, W. F., DiNola, A., Haak, J. R. (1984) Molecular dynamics with a coupling to an external bath. *J. Chem. Phys.,* **81***,* 3684-3690.
31. Bussi, G., Donadio, D., and Parrinello, M. (2007) Canonical sampling through velocity rescaling. *J. Chem. Phys.,* **126**, 014101.
32. Hess, B., Kutzner, C., van der Spoel, D., and Lindahl, E. (2008) GROMACS 4: Algorithms for Highly Efficient, Load-Balanced, and Scalable Molecular Simulation. *J. Chem. Theory Comput.,* **4**, 435-447.
33. Scott, W. R. P., Hünenberger, P. H., Tironi, I. G., Mark, A. E., Billeter, S. R., Fennen, J., Torda, A. E., Huber, T., Krüger, P., and van Gunsteren, W. F. (1999) The GROMOS Biomolecular Simulation Program Package. *J. Phys. Chem. A,* **103,** 3596-3607.
34. Spedding, H. (1962) Infrared Spectroscopy, in *Methods in Carbohydrate Chemistry. Vol. I. Analysis and preparation of sugars* (Whistler, R.L. and Wolfrom, M.L., eds.) Academic Press, New York, pp. 539-550.
35. Prado Fernandez, J., Rodríguez Vazquez, J. A., Tojo, E.,, and Andrade, J. M. (2003) Quantitation of λ-, ι-, and κ-carrageenan by midinfrared spectroscopy and PLS regresion. *Anal. Chim. Acta,* **480**, 23–37.
36. Stortz, C. A., and Cerezo, A. S. (1992) The ^{13}C NMR spectroscopy of carrageenans: calculation of chemical shifts and computer-aided structural determination. *Int. J. Biol. Macromol.*, **14***,* 237-242.
37. Noseda, M. D., and Cerezo, A. S. (1993) Room temperature, low-field ^{13}C-n.m.r. spectra of degraded carrageenans: Part III. Autohydrolysis of a lambda carrageenan and of its alkali-treated derivative. *Int. J. Biol. Macromol.*, **15***,* 177-181.

38. Cinelli, L. P., Andrade, L., Valente, A. P., and Mourão, P. A. S. (2010) Sulfated α-L-galactans from the sea urchin ovary: Selective 6-desulfation as eggs are spawned. *Glycobiology* **20**, 702–709.
39. Pereira, M. S., Vilela-Silva, E. S. A. C., Valente, A. P., and Mourão, P. A. S. (2002) A 2-sulfated, 3-linked α-L-galactan is an anticoagulant polysaccharide, *Carbohydr. Res.* **337,** 2231–2238.
40. Becker, C. F., Guimarães, J. A., Mourão, P. A. S., and Verli, H. (2007) Conformation of sulfated galactan and sulfated fucan in aqueous solutions: Implications to their anticoagulant activities. *J. Molec. Graph Modell.,* **26***,* 391–399.
41. Bock, K., and Pedersen, C. (1983) Carbon-13 nuclear magnetic resonance spectroscopy of monosaccharides. *Adv. Carbohydr. Chem. Biochem.,* **41***,* 27-66.
42. Zhuo, K., Liu, H., Zhang, X., Liu, Y., and Wang, J. (2008) A ^{13}C NMR study on the interactions of calcium chloride/potassium chloride with pyranosides in D_2O. *Carbohydr. Res.,* **343***,* 2428-2432.
43. Odonmažig, P., Ebringerová, A., Machová, E., and Alföldi, J. (1994) Structural and molecular properties of the arabinogalactan isolated from Mongolian larchwood (*Larix dahurica* L.). *Carbohydr. Res.,* **252***,* 317-324.
44. Ishii, T., Konishi, T., Ito, Y., Ono, H., Ohnishi-Kameyama, M., and Maeda, I. (2005) A β-(1 → 3)-arabinopyranosyltransferase that transfers a single arabinopyranose onto arabino-oligosaccharides in mung bean (*Vigna radiate*) hypocotyls. *Phytochemistry,* **66***,* 2418-2425.
45. Shashkov, A. S., Lipkind, G. M., Knirel, Y. A., and Kochetkov, N. K. (1988) Stereochemical factors determining the effects of glycosylation on the ^{13}C chemical shifts in carbohydrates. *Magn. Res. Chem.,* **26***,* 735-747.
46. Carroll, W. E. (1999) Thromboplastins, heparin, and polybrene. *Am. J. Clin. Pathol.,* **111**, 565.
47. Li, W., Johnson, D. J., Esmon, C. T., and Huntington, J. A. (2004) Structure of the antithrombin-thrombin-heparin ternary complex reveals the antithrombotic mechanism of heparin. *Nat. Struct. Mol. Biol.,* **11***,* 857-862.
48. Salvagnini, C., Michaux, C., Remiche, J., Wouters, J., Charlier, P., and Marchand-Brynaert, J. (2005) Design, synthesis and evaluation of graftable thrombin inhibitors for the preparation of blood-compatible polymer materials. *Org. Biomol. Chem.,* **3**, 4209-4220.
49. Fredenburgh, J. C., Stafford, A. R., and Weitz, J. I. (1997) Evidence for allosteric linkage between exosites 1 and 2 of thrombin. *J. Biol. Chem.,* **272**, 25493-25499.
50. Sheehan, J. P., and Sadler, J. E. (1994). Molecular mapping of the heparin-binding exosite of thrombin. *Proc. Natl. Acad. Sci. U.S.A.,* **91**, 5518-5522.
51. Matsubara, K., Matsuura, Y., Bacic, A., Liao, M.-L., Hori, K., and Miyazawa, K. (2001) Anticoagulant properties of a sulfated galactan preparation from a marine green alga, *Codium cylindricum. Int. J. Biol. Macromol.,* **28***,* 395-399.
52. Fernández, P. V., Estevez, J. M., Cerezo, A. S., and Ciancia, M. (2012) Sulfated β-D-mannan from the green seaweed *Codium vermilara*. *Carbohydr. Pol.,* **87**, 916-919.
53. Sommer-Knodsen, J., Bacic, A., and Clarke, A.E. (1998) Hydroxyproline-rich plant glycoproteins. *Phytochemistry,* **47***,* 483-497.
54. Somerville, C., Bauer, S., Brininstool, G., Facette, M., Hamann, T., Milne, J., Osborne, E., Paredez, A., Persson, S., Raab, T., Vorwerk, S., and Youngs, H. (2004) Towards a systems approach to understanding plant cell walls. *Science,* **306***,* 2206-2211.
55. Clarke, A. E., Anderson, R. L. and Stone, B. A. (1979). Form and function of arabinogalactans and arabinogalactan-proteins. *Phytochemistry* **18**, 521-540.
56. Tryfona, T., Liang, H-C., Kotake, T., Kaneko, S., Marsh, J., Ichinose, H., Lovegrove, A., Tsumuraya, Y., Shewry, P.R., Stephens, E., Dupree P. (2010) Carbohydrate structural analysis of wheat flour arabinogalactan protein. *Carbohydr. Res.*, **345***,* 2648-2656.
57. Uehara, T., Takeshita, M., and Maeda, M. (1992) Studies on anticoagulant-active arabinan sulfates from the green alga, *Codium latum*. *Carbohydr. Res.,* **23***,* 309–311.
58. Nilsson, S., and Piculell, L. (1991) Helix-Coil Transitions of Ionic Polysaccharides Analyzed within the Poisson-Boltzmann Cell Model. 4. Effects of Site-Specific Counterion Binding. *Macromolecules,* **24,** 3804-3811.
59. Robinson, G., Morris, E. R., and Rees, D. A. (1980) Role of double helices in carrageenan gelation: the domain model**.** *J. Chem. Soc., Chem. Comm.*, 152-153.

60. Aspinall G. O. (1982) Isolation and fractionation of Polysaccharides, in *The polysaccharides Vol. 1* (G. O. Aspinall , ed.). Academic Press, Orlando, Florida, pp.19-34.
61. Kelton J. G. and Warketin T. E. (2008) Heparin-induced thrombocytopenia: a historical perspective. *Blood*, **112**, 2607-2616.
62. Kam, P. C. A., Kaur, N., Thong, C. L. (2005) Direct thrombin inhibitors: pharmacology and clinical relevance. *Anaesthesia*, **60**, 565–574.
63. Di Nisio, N., Middeldorp, S., Büller, H. R. (2005). Direct thrombin inhibitors. *N. Eng.l J. Med.*, **353**, 1028-40.
64. Melo, F. R., Pereira, M. S., Foguel, D., and Mourão, A. S. (2004) Antithrommbin-mediated anticoagulant activity of sulfated polysaccharides. Different mechanisms for heparin and sulfated galactans. *J. Biol. Chem.*, **279**, 20824-20835.
65. Mao, W., Zang, X., Li, Y., and Zhang, H. (2006) Sulfated polysaccharides from marine algae *Ulva conglobata* and their anticoagulant activity. *A. Appl. Phycol.,* **18**, 9-14.

FOOTNOTES *This work was supported by grants from the National Research Council of Argentina, CONICET (PIP 559/2010) and ANPCYT (PICT 2008-0500) to MC, and Conselho Nacional de Desenvolvimento Científico e Tecnológico (CNPq), Fundação de Amparo a Pesquisa do Estado do Rio Grande do Sul (FAPERGS) and Coordenação de Aperfeiçoamento de Pessoal de Nível Superior (CAPES) to HV.
§Research Member of the National Research Council of Argentina (CONICET).
[1]To whom correspondence should be addressed: Cátedra de Química de Biomoléculas, Departamento de Biología Aplicada y Alimentos, Facultad de Agronomía, Universidad de Buenos Aires, Av. San Martín 4453, 1417 Buenos Aires, Argentina. Tel.: +54 11 4524-4042, Fax: +54 11 4524-8088. E-mail: ciancia@agro.uba.ar.
[2]Laboratorio de Hemostasia y Trombosis, Departamento de Química Biológica, Facultad de Ciencias Exactas y Naturales, Universidad de Buenos Aires, Ciudad Universitaria – Pabellón 2, C1428EHA Buenos Aires, Argentina.

[3]CIHIDECAR-CONICET, Departamento de Química Orgánica, Facultad de Ciencias Exactas y Naturales, Universidad de Buenos Aires, Ciudad Universitaria, Pabellón 2, C1428EHA Buenos Aires, Argentina.
[4]Instituto de Investigaciones Bioquímicas de Buenos Aires (IIBBA), CONICET, Av. Patricias Argentinas 435, 1405 Buenos Aires, Argentina.
[5]Programa de Pos-Graduação em Biologia Celular e Molecular, Centro de Biotecnologia, Universidade Federal do Rio Grande do Sul, Brasil.
[6]Faculdade de Farmácia, Universidade Federal do Rio Grande do Sul, Brasil.
[7]Instituto de Fisiología, Biología Molecular y Neurociencias (IFIByNE-CONICET), Facultad de Ciencias Exactas y Naturales, Universidad de Buenos Aires, Ciudad Universitaria – Pabellón 2, C1428EHA Buenos Aires, Argentina.
[8]The abbreviations used are: AT, antithrombin; HCII, heparin cofactor II; APTT, Activated Partial Thromboplastin Time; TT, Thrombin Time; MWCO, molecular weight cut off; WCOT, wall-coated open-tubular; HMQC, Heteronuclear Multiple Quantum Coherence; TMS, tetramethylsilane; MD, molecular dynamics; CD, circular dichroism; PT, Prothrombin Time; BT, bovine thrombin; HT: human thrombin; TB*O*, Orthochromatic Toluidine Blue; CB, Coomasie Blue; PPP, platelet poor plasma; RMSF, root mean square fluctuation; PDB, Protein Data Bank

FIGURE LEGENDS

FIGURE 1. HMQC spectra of (**A**) arabinan, **Ab1** and of **(B**) its desulfated derivative, **DAb1**.

FIGURE 2. Anticoagulant activity of **Ab1**. **A.** Direct inhibition of thrombin. **Ab1** inhibits thrombin (BT and HB) activity, even when AT and HCII are not present. Curves obtained from a partial non-competitive inhibition model fitted best to the inhibition data. **B.** Inhibition of BT activity mediated by AT and by HCII for increasing concentrations of **Ab1**.

FIGURE 3. Gel electrophoresis of **Ab1**, HT and formation of a complex. **A**. SDS-PAGE electrophoresis of **Ab1** and HT. **B.** Native electrophoresis of **Ab1** and HT, in conditions similar to those used in **A**. (*) Denote absence of either HT or **Ab1**.

FIGURE 4. Biophysical characterization of **Ab1**-HT interaction. **(A)** Fluorescence spectra of HT at increasing concentration of **Ab1**. (**B**) Fluorescence intensity measured at 345 nm at increasing concentration of **Ab1**. (**C**) Far-UV CD spectra of HT, **Ab1** and a mixture of HT and **Ab1.** The addition of the spectra measured for both isolated component is also shown.

FIGURE 5. Human (HT) and bovine (BT) thrombin profiles during MD simulations in their uncomplexed (black), persulfated arabinan octasaccharide-complexed at exosite 2 (red) and non-sulfated arabinan octasaccharide-complexed at exosite 2 (green) states. **A-B**, the root mean square fluctuation (RMSF) for the thrombin heavy chains are presented. In (**C**) and (**D**), the distances between the ND1 atom of His57 and OD1 atom of Asp102, which compose thrombin catalytic triad, are presented. In (**E**) and (**F**), the final arrangements of both studied octasaccharides, in relation to thrombin heavy chain, are shown (the protein light chain was omitted for clarity), together to the final state for thrombin catalytic triad and the enthalpic contribution for the interaction between the complete protein and carbohydrate chains.

Table 1. **Linkage analysis of pyranosic arabinans** [a,b]
The arabinans were permethylated and submitted to reductive hydrolysis and acetylation. The partially methylated alditol acetates were analyzed by GC-MS.

Monosaccharide	Structural Unit	Ab1	Ab2	DAb1
2,3,4-Ara[c]	L-Ara*p*(1→	0.7	6.2	3.3
2,4-Ara	→3) L-Ara*p* (1→	13.3	35.0	88.0
2-Ara	→3) L-Ara*p***4S** (1→	25.6	29.7	4.5
4-Ara	→3) L-Ara*p***2S** (1→	9.7	7.1	3.2
-	→3) L-Ara*p***2,4S** (1→	50.2	22.0	1.0

[a]Only derivatives of L-arabinose were detected. [b]Yield of the methylated derivative after discounting the added methoxy groups. Yield of methylation of **Ab1**, 65.2 %; of **Ab2**, 36 %, and of **DAb1**, 65.6 %. [c]2,3,4-Ara indicates 2,3,4-tri-*O*-methyl-L-arabinose, etc.

Table 2. Assignment of NMR spectra of the arabinan Ab1 and its desulfated derivative, DAb1[a]. Assignment was carried out by analysis of two-dimensional spectra and by comparison of the signals with those of related compounds.

	Chemical shift (ppm)				
Arabinan	**H1/C1**	**H2/C2**	**H3/C3**	**H4/C4**	**H5,H5'/C5**
DAb1	5.12/97.0	3.96/67.6	3.98/74.8	4.19/66.7	4.09,3.63/63.7
Ab1	5.37/95.5	4.59/78.8	4.36/70.8	4.87/75.4	4.07/61.6

[1]With reference to acetone, δ_{CH3} 2.175, 31.2, used as internal standard.

Table 3. Enthalpic contribution for the interaction between the amino acid residues of both HT and BT to disulfated and non-sulfated arabinan oligosaccharide.
Calculations were carried out by MD experiments.

Amino acid residues (HT/BT)	Enthalpic contribution for interaction (kJ/mol)			
	[L-Ara*p***2,4S-**(1→3)-L-Ara*p***2,4S**]$_4$		[L-Ara*p*-(1→3)-L-Ara*p*]$_4$	
	HT	*BT*	*HT*	*BT*
His91 / His91	-2 ± 2	-5 ± 9	-24 ± 7	-9 ± 6
Arg93 / Arg93	-133 ± 29	-101 ± 45	-12 ± 7	-2 ± 3
Arg97 / Lys97	-30 ± 41	0	0	0
Arg101 / Arg101	-93 ± 27	-51 ± 29	-7 ± 6	-3 ± 5
Arg126 / Lys126	-98 ± 30	-94 ± 46	0	0
Arg165 / Arg165	-39 ± 33	0	0	0
Arg233 / Arg233	-48 ± 34	-46 ± 33	-6 ± 5	-4 ± 8
Lys235 / Lys235	-58 ± 29	-3 ± 5	-2 ± 2	-1 ± 1
Lys236 / Lys236	-91 ± 38	-136 ± 43	-20 ± 12	-6 ± 8
Arg240 / Lys240	-17 ± 25	-125 ± 53	-20 ± 5	-18 ± 8
Gln244 / Arg244	0	-90 ± 61	-14 ± 8	-7 ± 11
SUB-TOTAL	**-570 ± 99**	**-650 ± 117**	**-104 ± 18**	**-49 ± 20**
TOTAL	**-740 ± 154**	**-698 ± 125**	**-333 ± 35**	**-297 ± 43**

Figure 1

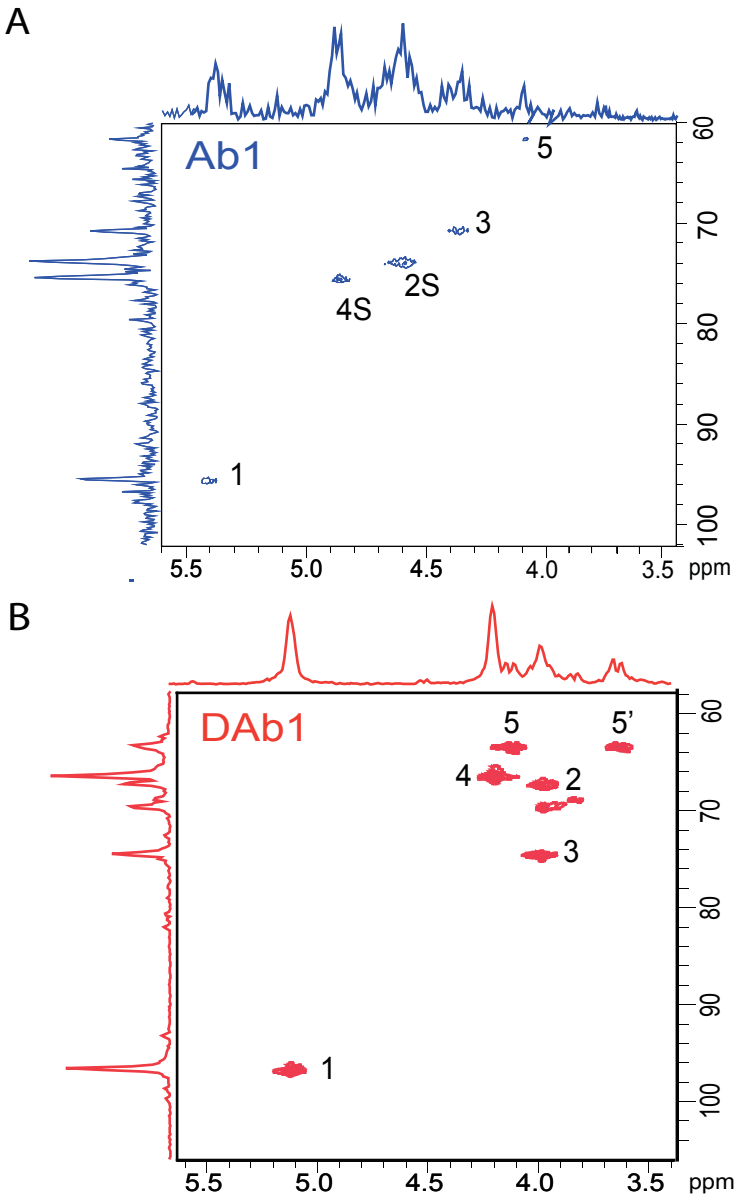

Figure 2

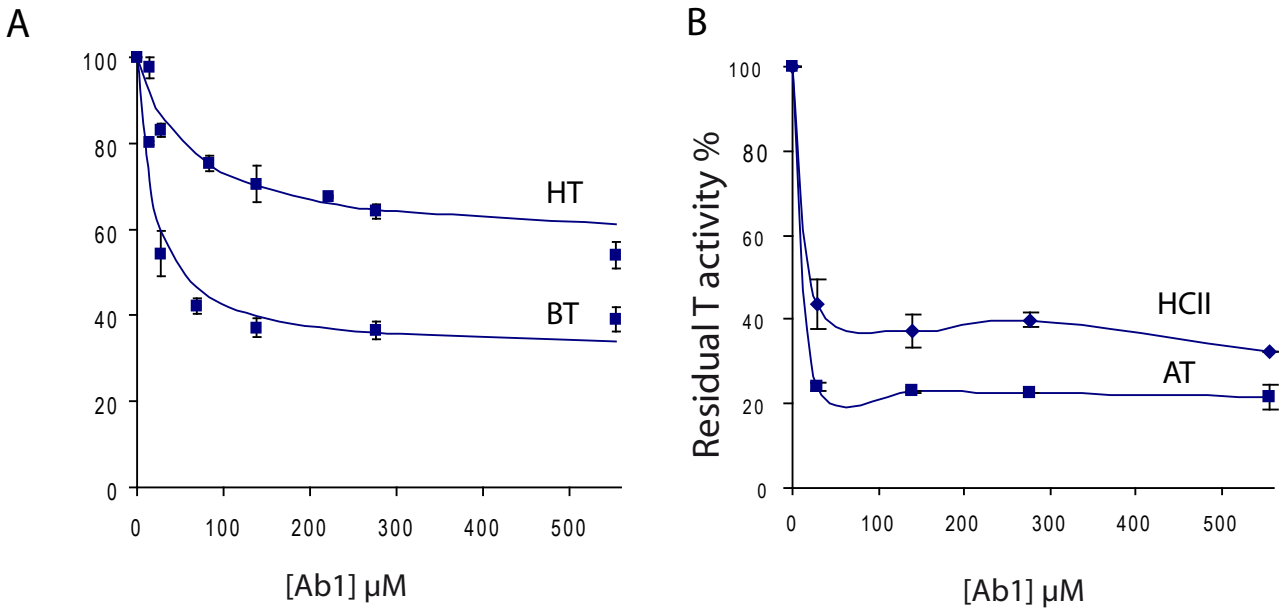

Figure 3

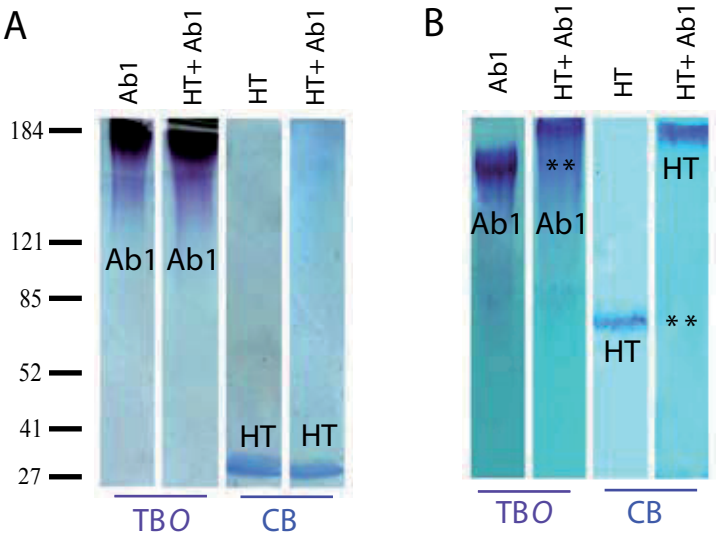

Figure 4

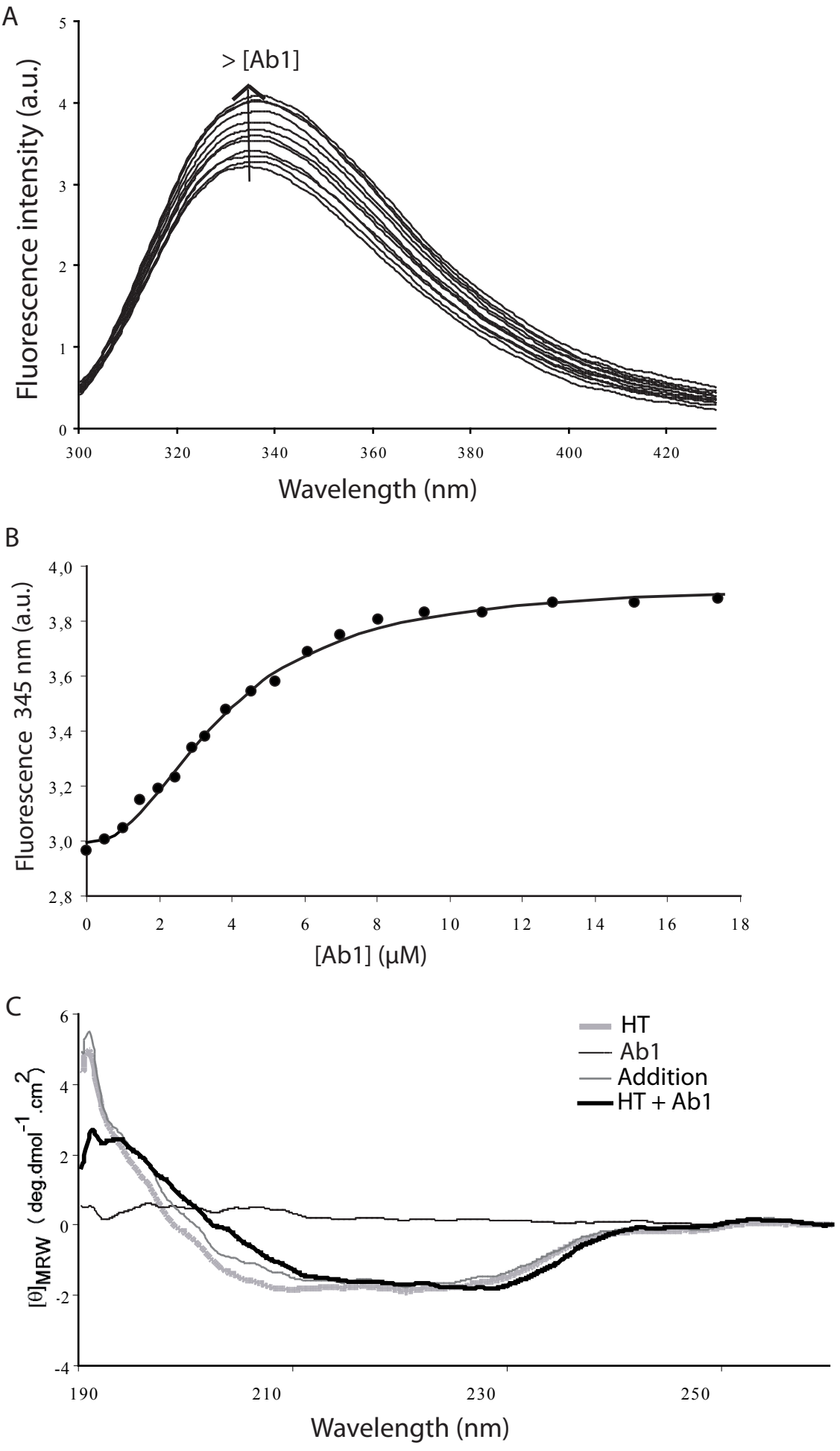

Figure 5